

# A nitrogen doped TiO<sub>2</sub> layer on Ti metal for the enhanced formation of apatite

Masami Hashimoto · Kazumi Kashiwagi · Satoshi Kitaoka

Received: 12 April 2011 / Accepted: 4 July 2011 / Published online: 16 July 2011  
© Springer Science+Business Media, LLC 2011

**Abstract** Biomedical titanium metals subjected to gas under precisely regulated oxygen partial pressures ( $P_{O_2}$ ) from  $10^{-18}$  to  $10^5$  Pa at 973 K for 1 h were soaked in a simulated body fluid (SBF), whose ion concentrations were nearly equal to those of human blood plasma, at 36.5°C for up to 7 days. The effect of oxygen partial pressures on apatite formation was assessed using X-ray diffraction (XRD), scanning electron microscopy (SEM) and X-ray photoelectron spectroscopy (XPS) measurements. After heating, the weight of the oxide layer (mainly TiO<sub>2</sub>) formed on the titanium metal was found to increase with increased oxygen partial pressure. Nitrogen (N)-doped TiO<sub>2</sub> (Interstitial N) was formed under a  $P_{O_2}$  of  $10^{-14}$  Pa. At lower  $P_{O_2}$  ( $10^{-18}$  Pa), only a titanium nitride layer (TiN and Ti<sub>2</sub>N) was formed. After soaking in SBF, apatite was detected on heat-treated titanium metal samples. The most apatite was formed, based on the growth rate calculated from the apatite coverage ratio, on the titanium metal heated under a  $P_{O_2}$  of  $10^{-14}$  Pa, followed by the sample heated under a  $P_{O_2}$  of 10 and  $10^4$  Pa (in N<sub>2</sub>). The titanium metal heated under a  $P_{O_2}$  of  $10^5$  Pa (in O<sub>2</sub>) experienced far less apatite formation than the former three titanium samples. Similarly, very little weight change was observed for the titanium metal heated under a  $P_{O_2}$  of  $10^{-18}$  Pa (in N<sub>2</sub>). During the experimental observation period (5 days,

36.5°C, SBF), the following relationship held: The growth rate of apatite decreased in the order  $P_{O_2}$  of  $10^{-14}$  Pa >  $P_{O_2}$  of 10 Pa ≥  $P_{O_2}$  of  $10^4$  Pa >  $P_{O_2}$  of  $10^5$  Pa >>  $P_{O_2}$  of  $10^{-18}$  Pa. These results suggest that N-doped TiO<sub>2</sub> (Interstitial N) strongly induces apatite formation but samples coated only with titanium nitride do not. Thus, controlling the formation of N-doped TiO<sub>2</sub> is expected to improve the bioactivity of biomedical titanium metal.

## 1 Introduction

Titanium and its alloy have been widely used as artificial joints, fracture fixation devices, and dental implants, because of their high fracture toughness and good biocompatibility. Titanium-based implants can not bond to the bone directly, since they are not bioactive. Therefore, in order to achieve high bioactivity, several methods have been developed such as chemical treatment with NaOH [1, 2] or H<sub>2</sub>O<sub>2</sub> [3, 4], sol-gel coating of titania layers, and the thermal oxidation and specific space techniques [5]. These treatments produce the Ti-OH group in a titania layer on the titanium surface, and it has been reported that the Ti-OH group provides a catalytic effect in triggering the heterogeneous nucleation of hydroxyapatite in simulated body fluid (SBF) [6, 7]. Sugino et al. [8] reported that two pieces of pure titanium covered with rutile produced via thermal oxidation at 400°C and set together in a V shape with varied mouth openings induced apatite formation on both facing surfaces in SBF when the open mouth spaces were approximately 600 μm. A pure titanium specimen with a machined macro-groove 500 μm in depth and 200–1000 μm in width thermally oxidized at 400°C also

M. Hashimoto (✉) · K. Kashiwagi · S. Kitaoka  
Japan Fine Ceramics Center, 2-4-1 Mutsuno, Atsuta-ku, Nagoya  
456-8587, Japan  
e-mail: masami@jfcc.or.jp

K. Kashiwagi  
e-mail: kashiwagi@jfcc.or.jp

S. Kitaoka  
e-mail: kitaoka@jfcc.or.jp

showed apatite formation in the internal space of the groove [8, 9]. These findings provide evidence that controlling both the appropriate specific spaces and the thermal oxidation temperature can enhance the potential for apatite formation on titanium. Kasuga et al. [10] reported the deposition of bone-like apatite on compacts of TiO<sub>2</sub> powders (80% anatase and 20% rutile) when they were irradiated with UV (500 W, Hg lamp) light in 1.5 SBF for 5 h at room temperature and subsequently held at 37°C for 5, 10 and 30 days. And also, Shozui et al. [11] reported that UV irradiation on thermally oxidized titanium enhanced the in vitro apatite forming ability. This enhanced apatite forming ability was attributed to an increase in the number of Ti–OH groups and surface free energy due to UV irradiation. However, the enhancement effect of the bioactivity by UV irradiation decreased over time. Furthermore, it is difficult to treat implants with complicated shapes uniformly.

It has been reported that TiO<sub>2</sub> might be positively charged in a reducing environment [12]. Therefore, it is possible that the N<sup>3-</sup> ion is concentrated near the surface of the TiO<sub>2</sub> layer. Thus, the properties of the TiO<sub>2</sub> interface may be controlled by incorporation of the N<sup>3-</sup> ion.

In this study, apatite formation was examined on well defined surfaces of TiO<sub>2</sub> formed on pure titanium, subjected to nitrogen gas under precisely regulated oxygen partial pressures (P<sub>O2</sub>), in SBF at 36.5°C. The dependence of apatite formation on the P<sub>O2</sub> was examined using quantitative spectroscopic and microscopic measurements.

## 2 Materials and methods

### 2.1 Preparation of materials

A sample of commercial pure Ti metal (Ti > 99.9%, Nilaco Co., Japan) 10 × 10 × 1 mm<sup>3</sup> was polished with a No. 400 diamond disk and then washed in acetone, 2-propanol and distilled water in an ultrasonic bath for 30 min. The Ti metal was placed in a furnace, the internal atmosphere of which was replaced with either N<sub>2</sub> (purity > 99.99995%), P<sub>O2</sub>-controlled N<sub>2</sub> using a solid-state electrochemical oxygen pump system or commercial air (purity > 99.99995%). Oxygen gas (purity > 99.999%) was used for comparison. The gas flow rate was 3 × 10<sup>-4</sup> m<sup>3</sup>/min. The sample was heated to 973 K from room temperature at a rate of 5 K/min, and then held at that temperature for 1 h, where the P<sub>O2</sub> value were 10<sup>-18</sup> and 10<sup>-14</sup> Pa for the controlled N<sub>2</sub>, 10 Pa for the commercial N<sub>2</sub>, 10<sup>4</sup> Pa for the commercial air and 10<sup>5</sup> Pa for O<sub>2</sub>. Finally, the sample was cooled back to room temperature at a rate of 5 K/min.

### 2.2 Surface characterization of the specimen after thermal treatment

The surfaces of the heat treated pure Ti were analyzed by thin film X-ray diffraction (TF-XRD) with a RINT Model 2000 spectrometer (Rigaku Denki Co. Ltd., Tokyo, Japan).

Surface chemical compositions of the outermost layers were analyzed using an X-ray photoelectron spectrometer (XPS) with an ULVAC-PHI microprobe (ULVAC PHI Inc., Tokyo, Japan). Aluminum K $\alpha$  radiation was used as the X-ray source. All binding energies were referenced to the carbon 1 s component set (284.5 eV). Overlapping peaks in the XPS spectra were separated by a computer-aided curve-deconvolution method.

Scanning electron microscopic (SEM) images of the surfaces and cross sections of heat treated pure Ti were obtained with an JEOL-6330F microscope (JEOL DATUM Co. Ltd., Nagoya, Japan) after gold treatment of the samples.

### 2.3 Evaluation of apatite forming ability

Simulated body fluid with ion concentrations (in mM: Na<sup>+</sup> 142, K<sup>+</sup> 5.0, Mg<sup>2+</sup> 1.5, Ca<sup>2+</sup> 2.5, Cl<sup>-</sup> 148, HCO<sub>3</sub><sup>-</sup> 4.2, HPO<sub>4</sub><sup>2-</sup> 1.0, SO<sub>4</sub><sup>2-</sup> 0.5) nearly equal to those of human blood plasma was prepared by dissolving NaCl, NaHCO<sub>3</sub>, KCl, K<sub>2</sub>HPO<sub>4</sub>, MgCl<sub>2</sub>·6H<sub>2</sub>O, CaCl<sub>2</sub> and Na<sub>2</sub>SO<sub>4</sub> in ion-exchanged water in a polystyrene bottle, according to the method described previously [7]. This solution was buffered at pH 7.4 with tris(hydroxymethyl)aminomethane ((CH<sub>2</sub>OH)<sub>3</sub>CNH<sub>2</sub>) and 1 M hydrochloric acid (HCl) at 36.5°C. The thermally treated specimens were soaked in 30 ml of SBF at 36.5°C for various periods of up to 7 days. The heat treated surface of the specimen was placed face down on the bottom of the polystyrene bottles. After soaking, the samples were removed from the solution, washed with distilled water gently, carefully dried and weighed using an electronic balance (resolution: 0.01 mg) to determine the apatite weight. The surfaces of the samples soaked in SBF were analyzed by TF-XRD and observed by SEM.

### 2.4 Apatite coverage measurement

Digital images of individual apatite particles were extracted from archival scanning electron micrographs. Apatite analysis was conducted by computer using a customized application based on public-domain image-processing (3D Volume, RATOC System, Tokyo, Japan) and analysis programs (Image J, National Institute of Health, Maryland, USA). Apatite particles were outlined using binary image processing and analyzed to obtain the area. The apatite coverage ratio (AR) was calculated using Eq. 1,

$$AR = (A/S) \times 100 \tag{1}$$

where  $A$  is the area of the apatite and  $S$  is the total area of the SEM image ( $8447 \mu\text{m}^2$ ).

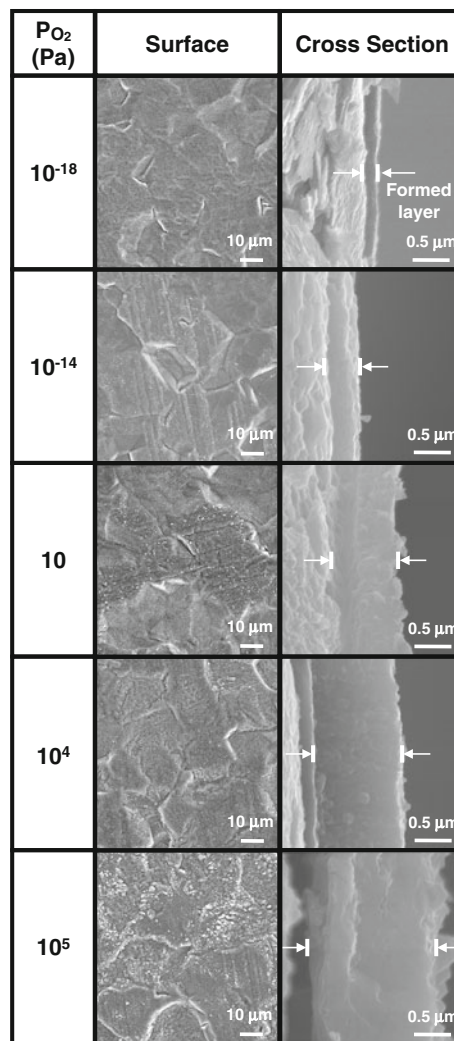
### 3 Results

#### 3.1 Characterization of heat-treated Ti metal

Figure 1 shows thin-film X-ray diffraction patterns of heat-treated Ti metal substrate. Two kinds of titanium nitride ( $\text{TiN}$  and  $\text{Ti}_2\text{N}$ ) phases were produced after heating under the lower  $P_{\text{O}_2}$  of  $10^{-18}$  Pa. By contrast, under the higher  $P_{\text{O}_2}$  ( $10^{-14}$ – $10^5$  Pa), only rutile-type  $\text{TiO}_2$  was detected. The peak intensities assigned to rutile increase with oxygen partial pressure.

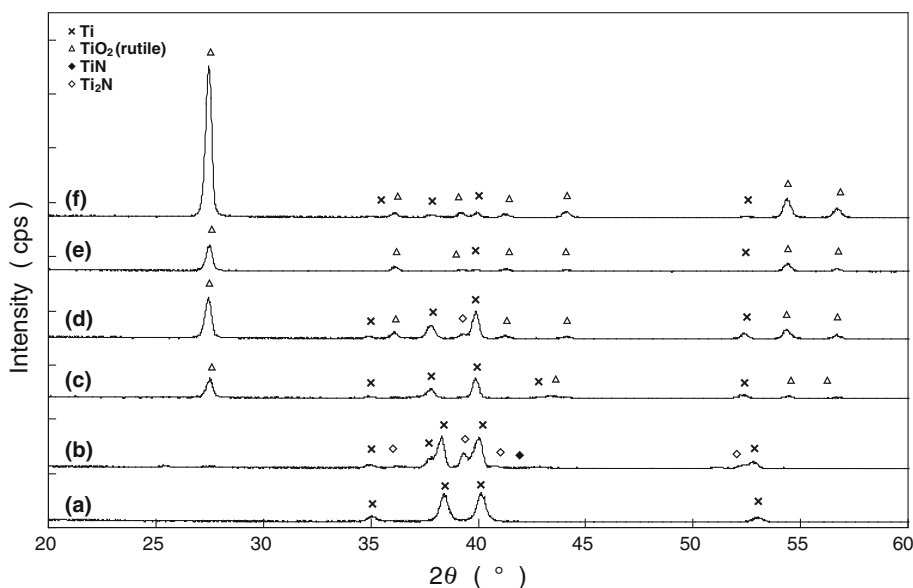
Figure 2 shows FE-SEM photographs of the surfaces and cross sections of pure Ti heated under various  $P_{\text{O}_2}$ . The layer formed under lower  $P_{\text{O}_2}$  ( $10^{-18}$  and  $10^{-14}$  Pa) was relatively smooth and its thickness was less than 1 micron. However, the surface roughness and layer thickness increased with an increase in  $P_{\text{O}_2}$ . The thickness of the layer formed under oxygen gas was at least 10 times that under a  $P_{\text{O}_2}$  of  $10^{-18}$  Pa. After heating, the weight of the layer formed was found to increase with increased oxygen partial pressure.

Figure 3 shows N1s and O1s XPS spectra of pure Ti heated under a  $P_{\text{O}_2}$  of  $10^{-18}$ – $10^5$  Pa. Under a  $P_{\text{O}_2}$  of  $10^{-18}$  Pa, a low-energy N1s peak at about 396 eV was detected, which corresponds to the Ti–N bonds in  $\text{TiN}$ , resulting from nitrogen substitution of oxygen in the  $\text{TiO}_2$  lattice. For samples heated under a  $P_{\text{O}_2}$  of  $10^{-14}$  Pa, a high-energy N1s peak is present at 401 eV. This corresponds to



**Fig. 2** SEM photographs of the surfaces and cross sections of pure Ti heated under various  $P_{\text{O}_2}$

**Fig. 1** Thin-film X-ray diffraction patterns of the surfaces of pure Ti (a) and those heated under various  $P_{\text{O}_2}$  at 973 K for 1 h:  $10^{-18}$  Pa (b),  $10^{-14}$  Pa (c), 10 Pa (d),  $10^4$  Pa (e) and  $10^5$  Pa (f)



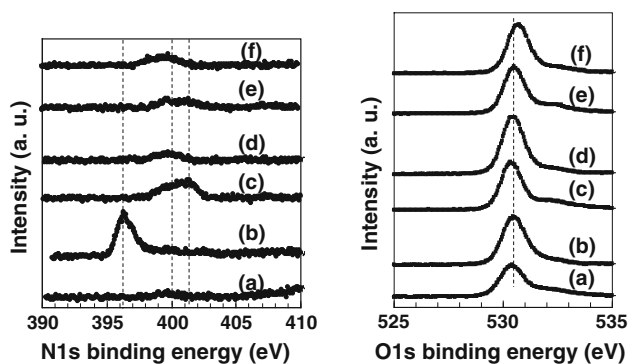


**Fig. 3** N1s and O1s XPS spectra of pure Ti (a) and Ti heated under various  $P_{O_2}$ :  $10^{-18}$  Pa (b),  $10^{-14}$  Pa (c), 10 Pa (d),  $10^4$  Pa (e) and  $10^5$  Pa (f)

oxidized nitrogen in a Ti–O–N structure, with the N atoms accommodated in the interstices of the  $TiO_2$  lattice and directly bonded to one or more  $O^{2-}$  ions. For samples heated under higher  $P_{O_2}$ , a high-energy N1s peak, corresponding to adsorbed nitrogen, is present at 400 eV. This peak could be due to  $N_2$  molecules in the atmosphere adsorbed on the surface. The binding energy of O1s (sample heated under a  $P_{O_2}$  of  $10^{-14}$  Pa) shift toward lower binding energy (around 0.1 eV). These results show that N-doped  $TiO_2$  (interstitial N) is formed on pure titanium heated under a  $P_{O_2}$  of  $10^{-14}$  Pa in a nitrogen atmosphere at 973 K.

### 3.2 Apatite formation on heat-treated Ti metal

Figure 4 shows thin-film X-ray diffraction patterns of heat treated Ti metal substrate after soaking in SBF for 7 days. After soaking in SBF, apatite was detected on the titanium

**Fig. 4** Thin-film X-ray diffraction patterns of pure Ti (a) and heat treated samples under various  $P_{O_2}$ :  $10^{-18}$  Pa (b),  $10^{-14}$  Pa (c), 10 Pa (d),  $10^4$  Pa (e) and  $10^5$  Pa (f) after being soaked in SBF at  $36.5^\circ\text{C}$  for 7 days

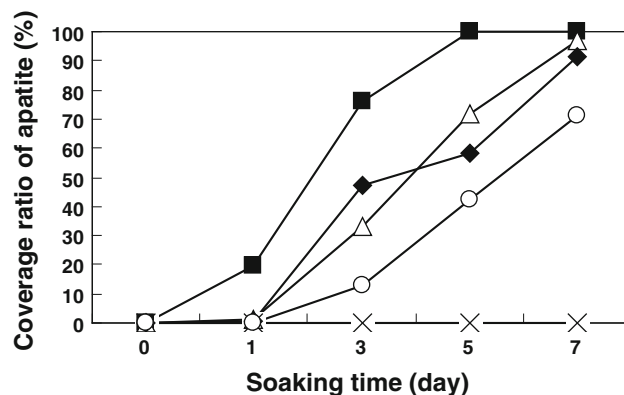
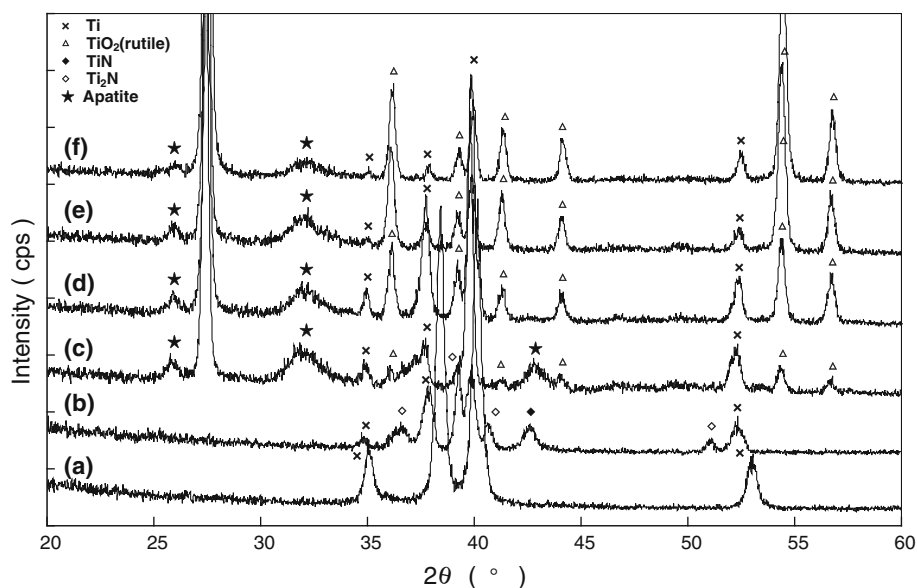


**Fig. 5** The dependence of soaking time in SBF on the apatite coverage ratio for pure Ti heated under various  $P_{O_2}$ :  $10^{-18}$  Pa (x),  $10^{-14}$  Pa (filled squares), 10 Pa (open triangles),  $10^4$  Pa (filled rhombuses) and  $10^5$  Pa (open circles)

heated under a  $P_{O_2}$  of  $10^{-14}$ – $10^5$  Pa. No apatite was detected on the titanium heated under a  $P_{O_2}$  of  $10^{-18}$  Pa.

Figure 5 shows the dependence of soaking time in SBF on the apatite coverage ratio for pure Ti heated under various  $P_{O_2}$ . Ignoring for a moment the titanium metal heated under a  $P_{O_2}$  of  $10^{-18}$  Pa, the apatite coverage ratio increased with soaking time. The titanium metal heated under a  $P_{O_2}$  of  $10^{-14}$  Pa (in  $N_2$ ) produced the highest apatite coverage ratio, which almost linearly increased with soaking time without an appreciable induction period, and reached a plateau after 5 days of soaking in SBF. The sample heated under a  $P_{O_2}$  of 10 (in  $N_2$ ) and  $10^4$  (in air) exhibited an induction period of almost 1 day but had an apatite coverage ratio which increased linearly beyond the induction period. The apatite coverage ratio of the titanium metal heated under a  $P_{O_2}$  of  $10^5$  Pa (in  $O_2$ ) was much lower than that of the former three samples. The following apatite

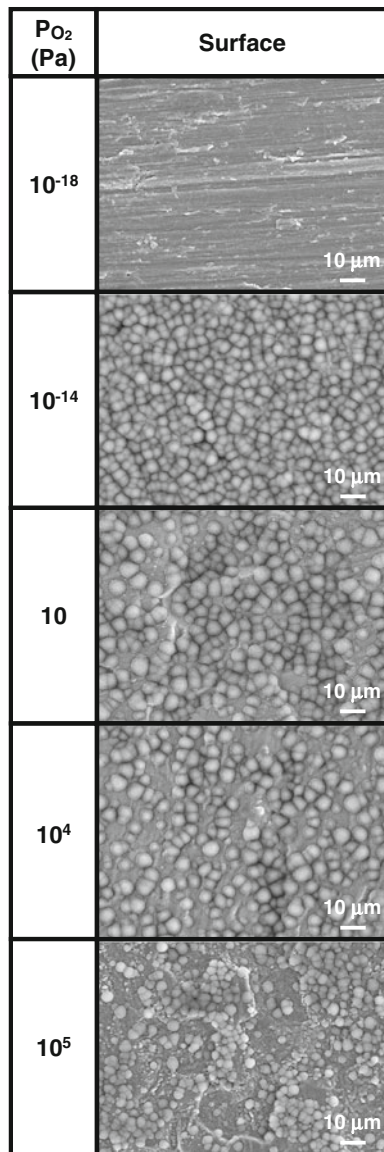


**Fig. 6** SEM photographs of the surfaces of pure Ti heated under various  $P_{O_2}$  after being soaked in SBF at 36.5°C for 5 days

coverage ratio following 5 days of soaking in SBF was obtained: 100% for the  $P_{O_2}$  of  $10^{-14}$  Pa, 72% for the  $P_{O_2}$  of 10 Pa, 58% for the  $P_{O_2}$  of  $10^4$  Pa and 42% for the  $P_{O_2}$  of  $10^5$  Pa. The most apatite was formed, based on the growth rate calculated from the coverage ratio of apatite, on the titanium metal heated under a  $P_{O_2}$  of  $10^{-14}$  Pa (in  $N_2$ ), followed by the sample heated under a  $P_{O_2}$  of 10 (in  $N_2$ ) and  $10^4$  Pa (in air).

Figure 6 shows scanning electron micrographs of the surfaces of the pure Ti heated under various  $P_{O_2}$  after soaking in SBF at 36.5°C for 5 days. No crystals were observed on the pure Ti heated under a  $P_{O_2}$  of  $10^{-18}$  Pa. The pure Ti heated under a  $P_{O_2}$  of  $10^{-14}$ , 10,  $10^4$  and  $10^5$  Pa were covered with hemispherical particles of apatite after 5 days of soaking in SBF. The particle size on the Ti

heated under a  $P_{O_2}$  of  $10^{-14}$  Pa was smaller than that of the three Ti samples heated under a  $P_{O_2}$  of 10,  $10^4$  and  $10^5$  Pa. All of the surfaces of the pure Ti heated under a  $P_{O_2}$  of  $10^{-14}$  Pa were covered with apatite, whereas the one heated under a  $P_{O_2}$  of 10,  $10^4$  and  $10^5$  Pa were not fully covered.

#### 4 Discussion

In this study, a new processed titanium surface to with enhanced bioactivity was proposed. Pure titanium was subjected precisely regulated oxygen partial pressures ( $P_{O_2}$ ) from  $10^{-18}$  to  $10^5$  Pa at 973 K for 1 h.

X-ray diffraction patterns (Fig. 1) and X-ray photoelectron spectra (Fig. 3) show that  $TiO_2$  was formed on the Ti samples heated under a  $P_{O_2}$  of 10,  $10^4$  and  $10^5$  Pa. Of special note, nitrogen doped  $TiO_2$  (interstitial N) was formed on the sample heated under a  $P_{O_2}$  of  $10^{-14}$  Pa. In contrast,  $TiN$  and  $Ti_2N$  were formed on the sample heated under a  $P_{O_2}$  of  $10^{-18}$  Pa. After soaking in SBF, apatite was formed on the samples except for the one heated under a  $P_{O_2}$  of  $10^{-18}$  Pa.

$TiO_2$  is known to promote surface apatite nucleation and to contain functional groups that are negatively charged at the crystallization pH. For example, the zeta potential of  $TiO_2$  has been reported to be  $-44.5$  mV at  $pH = 7.3-7.5$  in a phosphate-buffered saline solution [13]. This effect would result in the accumulation of cations, including calcium ions from the SBF on the Ti-OH groups of the  $TiO_2$ , thereby, inducing heterogeneous nucleation of apatite.

Quantitative measurements show that the apatite coverage ratio depended on the  $P_{O_2}$  (Fig. 5). The most potent apatite formation-inducing surface was the titanium metal heated under a  $P_{O_2}$  of  $10^{-14}$  Pa (nitrogen doped  $TiO_2$ ) which produced the highest coverage ratio of apatite within a short induction period, followed by the sample heated under a  $P_{O_2}$  of 10 and  $10^4$  Pa ( $TiO_2$ ) which exhibited a longer induction period. Compared with these samples heated in an  $N_2$  atmosphere, the one heated in an  $O_2$  atmosphere ( $P_{O_2}$ ,  $10^5$  Pa) ( $TiO_2$ ) was a weak apatite-inducing surface. The apatite formation was totally inhibited on the sample heated under a  $P_{O_2}$  of  $10^{-18}$  Pa ( $TiN$  and  $Ti_2N$ ). The potent apatite formation capability experimentally observed for nitrogen doped  $TiO_2$  with negatively charged group-bearing surfaces apparently proceed via complexation of a calcium ion with a surface negatively charged group, followed by subsequent complexation with phosphate ion. The coverage ratio of apatite (19.8%/day) for the nitrogen doped  $TiO_2$  ( $P_{O_2} = 10^{-14}$  Pa) was much higher than that for the  $TiO_2$  ( $P_{O_2} = 10$  and  $10^4$  Pa), soaked in SBF for one day (1.3 and 0.5%/day,

respectively). This implies that although spontaneous ion complexation is expected to occur irrespective of the presence of nitrogen doped TiO<sub>2</sub> or un-doped TiO<sub>2</sub> (P<sub>O<sub>2</sub></sub> = 10 and 10<sup>4</sup> Pa), subsequent phosphate ion adsorption or coordination on a Ca-surface nitrogen doped TiO<sub>2</sub> complex is greatly facilitated as compared to that of phosphate ion on a Ca-surface TiO<sub>2</sub> complex.

As for nitrogen doped TiO<sub>2</sub> formation in a reducing environment, the initial formation of TiO<sub>2</sub> may be followed by transformation to nitrogen doped TiO<sub>2</sub>. TiO<sub>2</sub> is positively charged in a reducing environment [12]. In this study, titanium metal was heated under a P<sub>O<sub>2</sub></sub> of 10<sup>-14</sup> Pa in a N<sub>2</sub> atmosphere. Therefore, the N<sup>3-</sup> ion was concentrated near the TiO<sub>2</sub> surface. Thus, the surface of N-doped TiO<sub>2</sub> might be more negative than that of TiO<sub>2</sub>. This highly negatively charged surface strongly induced apatite formation. Little apatite formation was induced for the TiN and Ti<sub>2</sub>N surfaces (P<sub>O<sub>2</sub></sub> = 10<sup>-18</sup> Pa) which may indicate that ion-induced dipole interactions between the Ti–N and Ca ion, the weakest of the inter-particle forces, do not participate in apatite nucleation.

## 5 Conclusions

N-doped TiO<sub>2</sub> was formed on Ti subjected to nitrogen gas under precisely regulated P<sub>O<sub>2</sub></sub> at 973 K. This N-doped TiO<sub>2</sub> surface might be more negative than that of TiO<sub>2</sub> because the N<sup>3-</sup> ion might be concentrated near the TiO<sub>2</sub> surface. The surface of N-doped TiO<sub>2</sub> acts as a potent substrate for apatite nucleation. The apatite formation predominantly occurs via calcium ion adsorption and complexation with a negatively charged group. The dependence of apatite formation on P<sub>O<sub>2</sub></sub> decreases in the order P<sub>O<sub>2</sub></sub> of 10<sup>-14</sup> Pa > P<sub>O<sub>2</sub></sub> of 10 Pa ≥ P<sub>O<sub>2</sub></sub> of 10<sup>4</sup> Pa > P<sub>O<sub>2</sub></sub> of 10<sup>5</sup> Pa >> P<sub>O<sub>2</sub></sub> of 10<sup>-18</sup> Pa.

**Acknowledgment** This work is supported in part by a Grant-in-Aid for society from Nagoya city to the Japan Fine Ceramics Center.

## References

1. Kim HM, Miyaji F, Kokubo T, Nakamura T. Preparation of bioactive Ti and its alloys via simple chemical surface treatment. *J Biomed Mater Res*. 1996;32:409–17.
2. Uchida M, Kim HM, Kokubo T, Fujibayashi S, Nakamura T. Effect of water treatment on the apatite-forming ability of NaOH-treated titanium metal. *J Biomed Mater Res (Appl Biomater)*. 2002;63:522–30.
3. Ohtsuki C, Iida H, Hayakawa S, Osaka A. Bioactivity of titanium treated with hydrogen peroxide containing metal chlorides. *J Biomed Mater Res*. 1997;35:39–47.
4. Wang XX, Hayakawa S, Tsuru K, Osaka A. A comparative study of in vitro apatite deposition on heat-, H<sub>2</sub>O<sub>2</sub>-, and NaOH-treated titanium surfaces. *J Biomed Mater Res*. 2001;54:172–8.
5. Wang XX, Yan W, Hayakawa S, Tsuru K, Osaka A. Apatite deposition on thermally and anodically oxidized titanium surfaces in a simulated body fluid. *Biomaterials*. 2003;24:4631–7.
6. Kokubo T, Kushitani H, Sakka S, Kitsugi T, Yamamuro T. Solution able to reproduce in vivo surface-structure changes in bioactive glass-ceramics A-W. *J Biomed Mater Res*. 1990;24:721–34.
7. Kokubo T, Takadama H. How useful is SBF in predicting in vivo bone bioactivity? *Biomaterials*. 2006;27:2907–15.
8. Sugino A, Uetsuki K, Tsuru K, Hayakawa S, Ohtsuki C, Osaka A. Gap effect on the heterogeneous nucleation of apatite on thermally oxidized titanium substrate. *Key Eng Mater*. 2008;361–363:621–4.
9. Sugino A, Uetsuki K, Tsuru K, Hayakawa S, Osaka A, Ohtsuki C. Surface topography designed to provide osteoconductivity to titanium after thermal oxidation. *Mater Trans*. 2008;49:428–34.
10. Kasuga T, Kondo H, Nogami M. Apatite formation on TiO<sub>2</sub> in simulated body fluid. *J Cryst Growth*. 2002;235:235–40.
11. Shozui T, Tsuru K, Hayakawa S, Osaka A. Enhancement of in vitro apatite-forming ability of thermally oxidized titanium surfaces by ultraviolet irradiation. *J Ceram Soc Japan*. 2008;116(4):530–5.
12. Ikeda JAS, Chiang YM. Space charge segregation at grain boundaries in titanium dioxide: I, relationship between lattice defect chemistry and space charge potential. *J Am Ceram Soc*. 1993;76(10):2437–46.
13. Wu W, Nancollas GH. Kinetics of heterogeneous nucleation of calcium phosphates an anatase and rutile surfaces. *J Col Interface Sci*. 1998;199:206–11.